1-2015

The mass profile and shape of bars in the Spitzer Survey of Stellar Structure in Galaxies (S4G) : search for an age indicator for bars.

Taehyun Kim
Seoul National University

Kartik Sheth
National Radio Astronomy Observatory

Dimitri A. Gadotti
European Southern Observatory

Myung Gyoon Lee
Seoul National University

Dennis Zaritsky
University of Arizona

See next page for additional authors

Original Publication Information

Kim, Taehyun, et al. "The Mass Profile and Shape of Bars in the Spitzer Survey of Stellar Structure in Galaxies (S4G): Search for an Age Indicator for Bars." 2015. *The Astrophysical Journal* 799(1): 10 pp.

The Astrophysical Journal, 799:99 (10pp), 2015 January 20 doi:10.1088/0004-637X/799/1/99

THE MASS PROFILE AND SHAPE OF BARS IN THE SPITZER SURVEY OF STELLAR STRUCTURE IN GALAXIES (S^{4}G): SEARCH FOR AN AGE INDICATOR FOR BARS

Taehyun Kim[1,2,3], Kartik Sheth[2], Dimitri A. Gadotti[3], Myung Gyoon Lee[1], Dennis Zaritsky[4], Bruce G. Elmegreen[5], E. Athanassoula[6], Albert Bosma[6], Benne Holwerda[7], Luis C. Ho[8,9], Sébastien Comerón[10,11], Johan H. Knapen[12,13], Joannah L. Hinz[14], Juan-Carlos Muñoz-Mateos[2,3], Santiago Erroz-Ferrer[12,13], Ronald J. Buta[15], Minjin Kim[16], Eija Laurikainen[10,11], Heikki Salo[10], Barry F. Madore[17], Jarkko Laine[10], Karín Menéndez-Delmestre[18], Michael W. Regan[19], Bonita de Swardt[20], Armando Gil de Paz[21], Mark Seibert[17], and Trisha Mizusawa[2,22]

[1] Astronomy Program, Department of Physics and Astronomy, Seoul National University, Seoul 151-742, Korea
[2] National Radio Astronomy Observatory/NAASC, 520 Edgemont Road, Charlottesville, VA 22903, USA
[3] European Southern Observatory, Casilla 19001, Santiago 19, Chile
[4] University of Arizona, 933 N. Cherry Avenue, Tucson, AZ 85721, USA
[5] IBM Research Division, T. J. Watson Research Center, Yorktown Heights, NY 10598, USA
[6] Aix Marseille Université, CNRS, LAM (Laboratoire d'Astrophysique de Marseille) UMR 7326, 13388 Marseille, France
[7] European Space Agency, ESTEC, Keplerlaan 1, 2200-AG, Noordwijk, Netherlands
[8] Kavli Institute for Astronomy and Astrophysics, Peking University, Beijing 100871, China
[9] Department of Astronomy, School of Physics, Peking University, Beijing 100871, China
[10] Division of Astronomy, Department of Physical Sciences, University of Oulu, Oulu, FIN-90014, Finland
[11] Finnish Centre of Astronomy with ESO (FINCA), University of Turku, Väisääntie 20, FI-21500, Piikkiö, Finland
[12] Instituto de Astrofísica de Canarias, E-38200 La Laguna, Tenerife, Spain
[13] Departamento de Astrofísica, Universidad de La Laguna, E-38205 La Laguna, Tenerife, Spain
[14] MMTO, University of Arizona, 933 N. Cherry Avenue, Tucson, AZ 85721, USA
[15] Department of Physics and Astronomy, University of Alabama, Box 870324, Tuscaloosa, AL 35487, USA
[16] Korea Astronomy and Space Science Institute, Daejeon 305-348, Korea
[17] The Observatories of the Carnegie Institution of Washington, 813 Santa Barbara Street, Pasadena, CA 91101, USA
[18] Universidade Federal do Rio de Janeiro, Observatório do Valongo, Ladeira Pedro Antônio, 43, CEP 20080-090, Rio de Janeiro, Brazil
[19] Space Telescope Science Institute, 3700 San Martin Drive, Baltimore, MD 21218, USA
[20] South African Astronomical Observatory, Observatory, 7935 Cape Town, South Africa
[21] Departamento de Astrofísica, Universidad Complutense de Madrid, Madrid 28040, Spain
[22] Florida Institute of Technology, Melbourne, FL 32901, USA
Received 2014 September 1; accepted 2014 November 13; published 2015 January 20

ABSTRACT

We have measured the radial light profiles and global shapes of bars using two-dimensional 3.6 μm image decompositions for 144 face-on barred galaxies from the Spitzer Survey of Stellar Structure in Galaxies. The bar surface brightness profile is correlated with the stellar mass and bulge-to-total (B/T) ratio of their host galaxies. Bars in massive and bulge-dominated galaxies (B/T > 0.2) show a flat profile, while bars in less massive, disk-dominated galaxies (B/T ~ 0) show an exponential, disk-like profile with a wider spread in the radial profile than in the bulge-dominated galaxies. The global two-dimensional shapes of bars, however, are rectangular/boxy, independent of the bulge or disk properties. We speculate that because bars are formed out of disks, bars initially have an exponential (disk-like) profile that evolves over time, trapping more disk stars to boxy bar orbits. This leads bars to become stronger and have flatter profiles. The narrow spread of bar radial profiles in more massive disks suggests that these bars formed earlier ($z > 1$), while the disk-like profiles and a larger spread in the radial profile in less massive systems imply a later and more gradual evolution, consistent with the cosmological evolution of bars inferred from observational studies. Therefore, we expect that the flatness of the bar profile can be used as a dynamical age indicator of the bar to measure the time elapsed since the bar formation. We argue that cosmic gas accretion is required to explain our results on bar profile and the presence of gas within the bar region.

Key words: galaxies: evolution – galaxies: formation – galaxies: spiral – galaxies: structure

1. INTRODUCTION

The presence and properties of galactic structures such as bars, bulges, rings, and spiral arms are not predetermined at the time of the galaxy formation. Both fast and slow ("secular") processes can create galactic structures and change their properties by a rearrangement of the mass, angular momentum, and energy with time (Athanassoula 2013; Sellwood 2014; also see reviews in Falcón-Barroso & Knapen 2013). As the merger rate in the universe declines, the evolution of galaxies at their late stages has increasingly been governed by secular evolution (Kormendy & Kennicutt 2004), stimulated by nonaxisymmetric structures such as bars, ovals, spiral structures, and triaxial dark matter halos. Among these, bars are one of the most important drivers of internal secular evolution in their host galaxies.

The nonaxisymmetric potential of a bar induces large-scale streaming motions in stars and gas into the central part of the galaxy (e.g., Athanassoula 1992a, 1992b; Sellwood & Wilkinson 1993). Being dissipative, the gas loses angular momentum and energy and flows inward toward the galactic center (Knapen et al. 1995; Regan et al. 1999; Sheth et al. 2000, 2002), accumulating in the central $\sim$1 kpc of galaxies (e.g., Sakamoto et al. 1999; Sheth et al. 2005). The accumulation of gas in the central parts leads to high levels of circumnuclear star formation activity (Sérsic & Pastoriza 1965; Hawarden et al. 1986; Devereux 1987; Martin 1995; Ho et al. 1997; Sheth et al. 2000, 2005; Gadotti & dos Anjos 2001; Ellison et al. 2011; Coelho & Gadotti 2011; Wang et al. 2012); this circumnuclear star formation is often in the shape of nuclear rings (Knapen et al. 2002; Comerón et al. 2010; Kim et al. 2012; Seo & Kim 2013)

and nuclear star clusters (Böker et al. 2002, 2004, 2011). Such star formation activities may help to create disky pseudobulges (Kormendy & Kennicutt 2004; Sheth et al. 2005; Athanassoula 2005; Debattista et al. 2006). Bars are the primary mechanism for transporting gas from a few kiloparsec scale to the central kiloparsec. However, there have been mixed answers to the question of whether the presence of a bar and active galactic nucleus (AGN) activity are connected. Some studies find weak statistical links among AGN activity and the presence of bars (e.g., Arsenault 1989; Knapen et al. 2000; Laine et al. 2002; Laurikainen et al. 2004a; Coelho & Gadotti 2011), whereas others find little or no link (e.g., Moles et al. 1995; McLeod & Rieke 1995; Mulchaey & Regan 1997; Ho et al. 1997; Hunt & Malkan 1999; Martini et al. 2003; Lee et al. 2012; Cisternas et al. 2013). While bar torques drive gas inside the bar corotation inward, they push the gas between the corotation and outer Lindblad resonance (OLR) outward (Combes 2008; Kubryk et al. 2013).

Bars have been reported to change the chemical abundance gradient in the disk, presumably as a result of large-scale streaming motions induced by the bar (e.g., Zaritsky et al. 1994; Martin & Roy 1994; Dutil & Roy 1999; but also see Pérez & Sánchez-Blázquez 2011; Sánchez et al. 2012, 2014). Bars may change the chemical abundance gradient inside the corotation radius, but they seem to have only a small impact outside the bar itself. Bars may redistribute stars in the galaxy disk, leading to disk breaks in the disk profile (e.g., Debattista et al. 2006; Radburn-Smith et al. 2012; Muñoz-Mateos et al. 2013; Kim et al. 2014, hereafter Paper I). Bars drive the formation of inner rings and outer rings (Buta & Combes 1996; Buta et al. 2003; Romero-Gómez et al. 2006; Athanassoula et al. 2009a, 2009b) and possibly spiral density waves (Buta et al. 2009; Salo et al. 2010). Simulations show that bars may evolve over time by transferring angular momentum from the baryons to the outer disk and/or halo (Sellwood 1980; Debattista & Sellwood 1998; Athanassoula 2002, 2003; Valenzuela & Klypin 2003; Martinez-Valpuesta et al. 2006; Begelman & Shlosman 2009; Saha et al. 2012). As bars lose angular momentum, their corotation radius moves outward, and they become longer and thinner (Athanassoula 2003, 2013). Bars thus play an important role in secular evolution of galaxies by redistributing the energy, angular momentum, and mass across the disk.

Bar properties change along the Hubble sequence. Early Hubble-type disks (earlier than SBb) have longer bars, both in an absolute sense and relative to their disks, compared to late Hubble-type disk galaxies (later than SBb; Elmegreen & Elmegreen 1985; Martin 1995; Laurikainen & Salo 2002; Laurikainen et al. 2004a, 2007; Erwin 2005; Menéndez-Delmestre et al. 2007; Marinova & Jogee 2007). Bars in early-type spirals tend to show uniform intensity along the major axis of the bar, i.e., a flat radial light profile compared to the interbar region, whereas bars in late-type spirals tend to have exponential radial profiles (Elmegreen & Elmegreen 1985; Baumgart & Peterson 1986; Elmegreen et al. 1996; Regan & Elmegreen 1997). Flat bars are associated with two-arm grand design spirals. However, exponential bars have multiple spirals or flocculent spirals (Elmegreen & Elmegreen 1985), and these spirals are often not physically connected directly to the bar structure. As bars evolve, stellar orbits of bars also evolve (Athanassoula 2013). Thus, they may be different between early- and late-type disk galaxies. Such orbits define the outermost two-dimensional (2D) shape of bars. Therefore, if we investigate both bar profile and shape over Hubble type, and as a function of structural properties of galaxies, we should be able to better understand how bars evolve.

Previous studies have analyzed at most a few dozen bars with relatively simple (one-dimensional) analysis of their light profile. Although some galaxies have been analyzed using 2D decompositions including bar components (e.g., Laurikainen et al. 2004b, 2011; Gadotti 2009; Vika et al. 2012), properties of bars have not yet been studied in detail. With the Spitzer Survey of Stellar Structure in Galaxies (S^4G; Sheth et al. 2010), we now have the opportunity to measure the bar light profile, the bar shape, and bulge and disk properties using the survey of 3.6 μm images, which are less affected by dust, in a sizable sample of galaxies shedding light on the evolution of bars and disks. The large, uniform, and homogenous 3.6 μm data give us a virtually dust-free view of stellar structures, which is important because dust can affect the measurement of galactic structures (e.g., Holwerda et al. 2005; Gadotti et al. 2010; Fathi et al. 2010; Kelvin et al. 2012; Pastrav et al. 2013).

As bars and bulges are embedded in disks, structural properties of bars are best studied through 2D decompositions (e.g., de Jong 1996; Laurikainen et al. 2005, 2007, 2010; Gadotti 2008, 2009; Durbala et al. 2008, Paper I). A shortcoming for most of the previous studies has been the use of a fixed profile for the bar and of a single exponential for the disk. Although several studies have tried to fit bars with a Sérsic or Ferrers function (e.g., Laurikainen et al. 2005, 2010; Weinzirl et al. 2009; Vika et al. 2012; Lansbury et al. 2014), light profiles of bars have not been examined. Moreover, a majority of disk galaxies have a disk break (Pohlen et al. 2002; Erwin et al. 2005; Pohlen & Trujillo 2006; Erwin et al. 2008; Gutiérrez et al. 2011; Maltby et al. 2012a; Comerón et al. 2012; Martín-Navarro et al. 2012; Muñoz-Mateos et al. 2013; Laine et al. 2014); therefore, it is critical to fit both the inner and outer disks (Paper I). The disk break affects the measurement of the structural properties of the bar, bulge, and disk. For example, in down-bending (Type II) disks, we find that B/T and bar-to-total (Bar/T) can change up to 10% and 25%, respectively (Paper I). The disk scale length and central surface brightness of the disk also change once the disk break is properly modeled. However, none of the previous studies consider disk breaks in measuring structural properties of galaxies. In this work we allow the bar profile to vary and fit the disk break in 144 galaxies from S^4G. The radial profile and global shape of bars are analyzed with respect to the bulge and disk properties, with an aim of understanding the evolution of disks.

The paper is organized as follows. In Section 2 we give a brief overview of our sample selection and describe our 2D image decomposition procedure. We explore the radial surface brightness profile of the bar in Section 3. Global shapes of bars are examined in Section 4. We discuss our results in Section 5, and we summarize and conclude in Section 6.

2. DATA AND DATA ANALYSIS

We refer the reader to Paper I for details on the sample selection and the 2D decomposition methodology, and we briefly summarize the data set and analysis here.

2.1. Data

We use data from S^4G (Sheth et al. 2010), a survey of 2352 nearby galaxies using the Infrared Array Camera (IRAC; Fazio et al. 2004) at 3.6 and 4.5 μm. Mid-infrared (MIR) data are a good tracer of the stellar mass distribution in galaxies,

because they are less hampered by dust with only a small local contamination from asymptotic giant branch stars or hot dust around red supergiants (Meidt et al. 2012a, 2012b). Thus, in this study we made use of 3.6 μm images that form an ideal data set for exploring properties of stellar bars.

Our sample of 144 barred galaxies are all the barred galaxies from the data that had been processed by the S^{4}G pipelines (Pipelines 1, 2, and 3; Sheth et al. 2010) at the beginning of this study in 2011 November. Properties of galaxies are presented in Paper I. The bar classification was first done visually by K. Sheth, T. Kim, and B. de Swardt, and then later the presence of a bar was confirmed by comparing with the MIR classification (Buta et al. 2010, 2014). According to this MIR classification, there are ~800 strongly barred (SB) galaxies and ~370 weakly barred (SAB) galaxies in the full sample of the S^{4}G.

2.2. Data Analysis

We performed 2D decompositions on 3.6 μm images from S^{4}G using the BUlge Disk Decomposition Analysis code (BUDDA v2.2, Gadotti 2008; de Souza et al. 2004) and fit each galaxy with a disk, a bar, a bulge, and, if present, a central point source. As noted earlier, the majority of disks have a change of slope in their radial light distribution with either down-bending (Type II) or up-bending (Type III) profiles (Pohlen & Trujillo 2006; Hunter & Elmegreen 2006; Erwin et al. 2008; Gutiérrez et al. 2011; Maltby et al. 2012b; Muñoz-Mateos et al. 2013; Laine et al. 2014). Owing to the disk breaks, disks have inner and outer disk scale lengths that differ in the median by 40% (Paper I) and lead to differences of ~10% in B/T and ~25% in Bar/T in the decompositions.

We follow the procedures detailed in Paper I but summarize the fitting procedures of bars here. The bar surface brightness profile is also modeled with the Sérsic profile (Sérsic 1963),

$$\mu_{\rm bar}(r) = \begin{cases} \mu_{e,\rm bar} + c_{n,\rm bar}\left[\left(\frac{r}{r_{e,\rm bar}}\right)^{1/n_{\rm bar}} - 1\right], & \text{if } r \leqslant r_{\rm bar} \\ 0, & \text{if } r > r_{\rm bar} \end{cases} \quad (1)$$

where $c_{n,\rm bar} = 2.5(0.868n_{\rm bar} - 0.142)$ and $r_{\rm bar}$ is the radius of the bar along the major axis. Beyond this radius the light profile of the bar is truncated to zero level in the model images.

The global shape of each component can be modeled with generalized ellipses (Athanassoula et al. 1990),

$$\left(\frac{|x|}{a}\right)^c + \left(\frac{|y|}{b}\right)^c = 1, \quad (2)$$

where x and y are positions of points, a and b are semimajor and semiminor axis, respectively, and c is the shape parameter that describes the shape of the ellipse. If $c = 2$, then the shape of the component is a perfect ellipse. If $c < 2$, then the shape of the component is disky, while if $c > 2$, the shape of the component is boxy. In this study, we only characterize the shape of a bar component, and we fix the shape parameter ($c = 2$) for the disk and bulge.

In case a nuclear point source is present (23/144, 16% of the sample), we model it with a point-spread function profile with its appropriate FWHM, while we fit only for the peak intensity. Possible candidates of nuclear sources are nonstellar emission from AGNs, nuclear star clusters, and unresolved small bulges. The lowest B/T that we obtain is 0.004. This is the lower limit at which we can identify a bulge visually from our analysis. In our sample, there are a number of bulgeless galaxies. Before we run BUDDA, we visually inspect the images and radial light profiles of the galaxies, and if a galaxy does not have a bulge, then we only fit these galaxies with a disk and a bar; thus, such galaxies have B/T = 0. In this study, by "bulgeless" we refer to the galaxies without a classical or a disky pseudobulge. But still, bulgeless galaxies can have a boxy/peanut feature, which is sometimes called a boxy/peanut bulge (For details, readers are referred to Athanassoula 2005; Athanassoula & Beaton 2006).

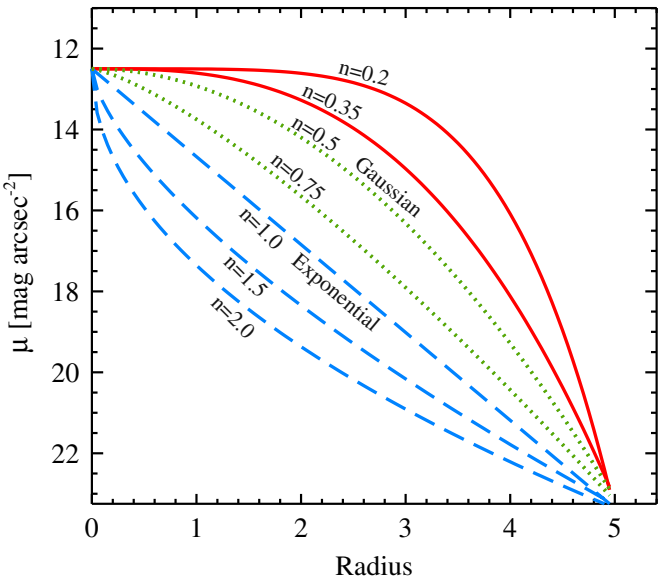

Figure 1. Schematic plot of Sérsic profiles that describe various radial surface brightness profiles of bars. Radial profiles of $n = 0.2$–2 are presented. Gaussian ($n = 0.5$) and exponential ($n = 1.0$) profiles are also shown. Flat profiles are in red, intermediate profiles are in green, and exponential steep profiles are in blue. Radius is in an arbitrary unit.

3. SURFACE BRIGHTNESS PROFILE OF BARS

3.1. Bar Profiles Fitted with the Sérsic Function

We use Sérsic indices to measure the steepness of the light profile of a bar. Surface brightness profiles with different Sérsic indices from $n = 0.2$ to 2.0 are shown in Figure 1. In Figure 2(a) we plot bar Sérsic indices ($n_{\rm bar}$) as a function of the absolute magnitude of the galaxy. The 3.6 μm magnitudes are converted to a stellar mass following the method outlined in Appendix A of Muñoz-Mateos et al. (2013), which is based on the mass-to-light ratio measurement from Eskew et al. (2012). Figure 2(b) shows the distributions of galaxies that have a flat bar, an intermediate bar, and an exponential bar. We find that massive galaxies predominantly have flat bars ($n_{\rm bar} < 0.4$), while less massive galaxies primarily have exponential "disk-like" bars ($n_{\rm bar} \geqslant 0.8$), although some low-mass galaxies show flat bars. The transition from having predominantly flat bars to more exponential bars occurs around $M_{3.6} \sim -20$ AB mag ($\sim M_*/M_\odot \sim 10^{10.2}$).

Next we plot the distribution of $n_{\rm bar}$ in Figures 3(a) and (b), now dividing the galaxies based on the bulge dominance: in red we show the bulge-dominated galaxies with a B/T[23] > 0.2,[23] in orange we show the intermediate cases with $0.0 < {\rm B/T} \leqslant 0.2$, and in blue we show the disk-dominated systems with B/T = 0. The arrows at the top of the panel indicate the median $n_{\rm bar}$ for

[23] B/T is from our own 2D decompositions using 3.6 μm images.

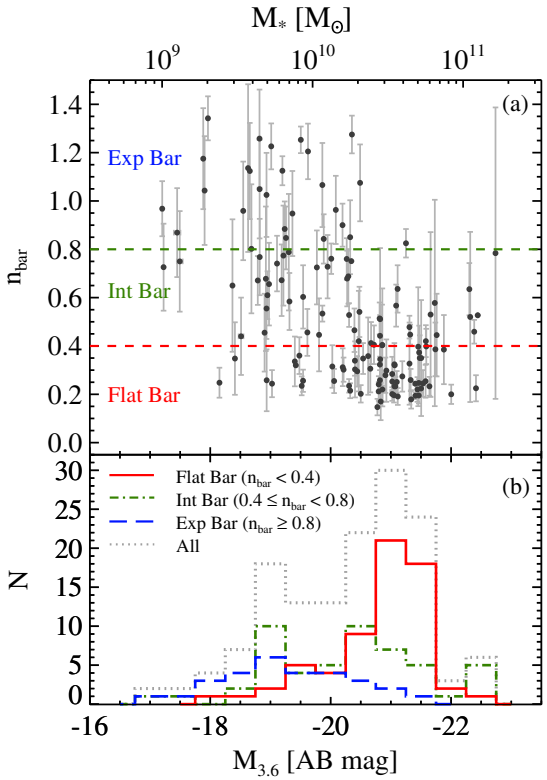

Figure 2. (a) Bar Sérsic indices as a function of absolute magnitude of galaxies. Stellar masses, converted from absolute magnitude of galaxies, are shown on top. Error bars are statistical 1σ uncertainty errors for Sérsic indices. (b) Distributions of absolute magnitudes of galaxies having flat bars ($n_{\rm bar} < 0.4$) in red solid line, intermediate bars ($0.4 \leqslant n_{\rm bar} < 0.8$) in green dot–dashed line, and exponential bars ($n_{\rm bar} \geqslant 0.8$) in blue dashed line.

each group. The main point to note is that the distributions of $n_{\rm bar}$ of the three groups are different. Bulge-dominated galaxies have a smaller $n_{\rm bar}$ with a median bar Sérsic index, $\langle n_{\rm bar}\rangle \sim 0.30$, whereas disk-dominated systems span a wide range of bar Sérsic index from 0.25 to 1.4, with a median $\langle n_{\rm bar}\rangle \sim 0.85$. The majority of exponential bars are in bulgeless galaxies, and all galaxies with $n_{\rm bar} > 0.7$ are bulgeless galaxies. Thus, bar profiles can be better separated by bulge dominance and bulge types than by galaxy mass.

Next, we investigate the bar Sérsic index versus the bulge Sérsic index. We divide the bulge light profiles into three groups: no bulge ($n_{\rm bulge} = 0$), disky pseudobulge[24] ($0 < n_{\rm bulge} \leqslant 2.0$), and a classical bulge ($n_{\rm bulge} > 2.0$) following the separation of Fisher & Drory (2008).

The bar Sérsic index distribution for these groups is shown in Figure 3(b). We find that classical bulge galaxies have a smaller $n_{\rm bar}$ and show a flatter bar profile compared to bulgeless galaxies. In Figure 3(c) we plot the different bar profiles, but now we overplot the median bar profiles for galaxies with a classical bulge with the red solid line, galaxies with a disky pseudobulge with the green dashed line, and bulgeless galaxies with the blue short-dashed line. There does seem to be a progression of $n_{\rm bar}$, but the samples are still not large enough to get a statistically significant difference in the distribution of the bar profiles between the classical and disky pseudobulge groups. Nevertheless, the basic conclusion from these figures is that the bulge-dominated galaxies and especially those with a classical bulge have the flattest bars, and this is consistent with the early findings of Elmegreen & Elmegreen (1985).

We check how $n_{\rm bar}$ vary with bar length ($L_{\rm bar}$) and normalized bar length ($L_{\rm bar}/R_{25.5}$) in Figure 4.[25] We find that longer bars tend to show flatter profiles (Figure 4(a)). This is in line with the previous studies (e.g., Elmegreen & Elmegreen 1985; Baumgart & Peterson 1986), considering that early-type galaxies have longer bars (e.g., Erwin 2005; Laurikainen et al. 2007; Menéndez-Delmestre et al. 2007). However, when lengths of bars are normalized to $R_{25.5}$, the correlation is not clear (Figure 4(b)).

For highly inclined galaxies, projection effects could be such that bulge light is mixed with the bar, complicating the decomposition. Nevertheless, this effect is unlikely to influence much in our sample, because we select our samples to have mild inclination ($i < 60$). The mean of the bulge effective radii to bar ratio ($\langle r_{\rm eff,bulge}/r_{\rm bar}\rangle$) is 7.5 for galaxies with a bulge. Thus, bars span a large enough area compared to bulges, enabling us to well estimate bar Sérsic indices.

3.2. Fitting Bar Model Images with the Modified Ferrers Profile

We model the bar profile with the Sérsic profile that is provided by BUDDA to fit bars. However, bars also have been modeled with the Ferrers function (e.g., Laurikainen et al. 2007,

[24] In this paper, by "disky pseudobulge", we specifically refer to a disk-like or disky bulge and do not include boxy/peanut features that are thick parts of the bar. See Athanassoula (2005), Athanassoula & Beaton (2006) for details.

[25] Radius at $\mu_{3.6\,\mu{\rm m}} = 25.5$ AB mag arcsec^{-2} from the S^{4}G Pipeline 3.

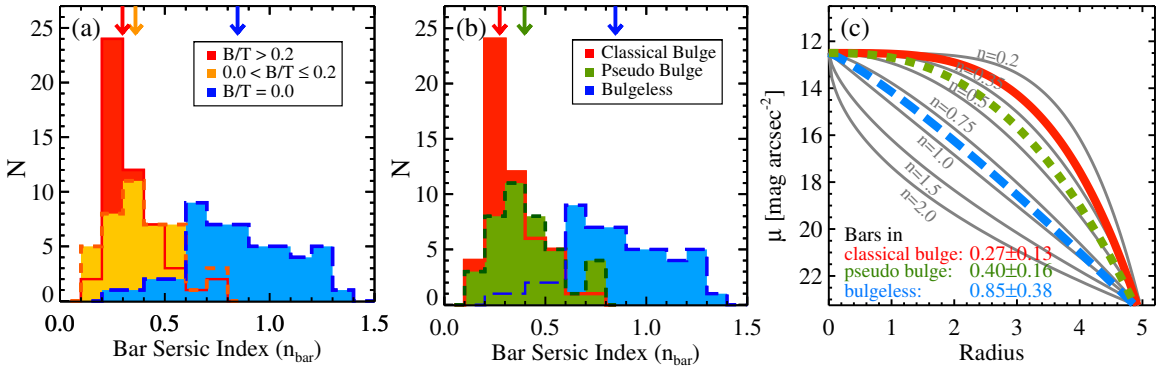

Figure 3. Distribution of bar Sérsic indices. (a) The sample is divided into three groups: galaxies with $B/T > 0.2$, $0 < B/T \leqslant 0.2$, and $B/T = 0$. Downward-pointing arrows indicate median bar Sérsic indices for each group. (b) The sample is split into galaxies with a classical bulge, galaxies with a disky pseudobulge, and bulgeless galaxies. Galaxies that have a bulge component have smaller bar Sérsic indices than bulgeless galaxies, which implies that galaxies that have a bulge have flatter bars than bulgeless galaxies. (c) Median bar profiles of classical bulge galaxies (red solid line), disky pseudobulge galaxies (green dashed line), and bulgeless galaxies (blue short-dashed line) are plotted. Median Sérsic indices are also shown on the bottom.

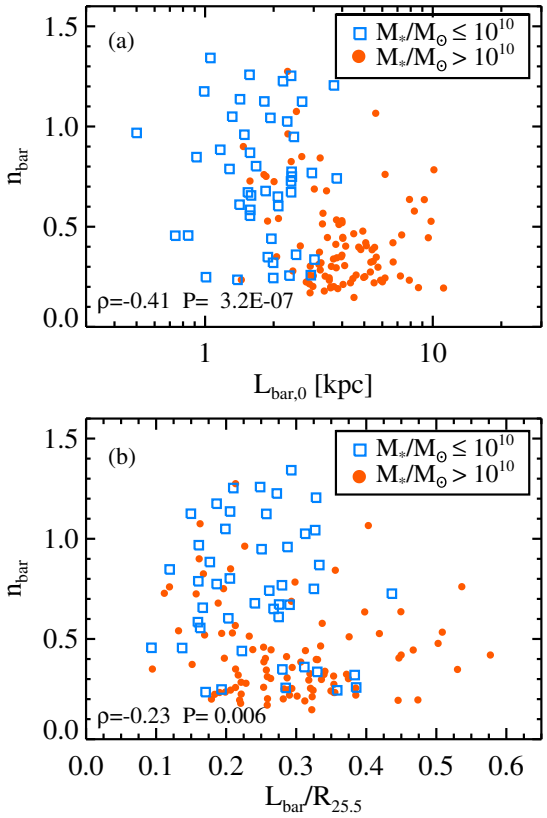

Figure 4. (a) Bar Sérsic indices ($n_{\rm bar}$) with bar lengths ($L_{\rm bar}$); (b) $n_{\rm bar}$ with normalized bar lengths ($L_{\rm bar}/R_{25.5}$). Massive galaxies are plotted by circles, while less massive galaxies are plotted by squares. Spearman's rank correlation coefficient (ρ) and significance are presented in the lower left corner of each panel.

2010; Peng et al. 2010). The Ferrers function has the following functional form:

$$\mu_{\rm bar}(r) = \mu_0(1-(r/r_{\rm out})^2)^{m_{\rm bar}+0.5}, \quad (3)$$

where $m_{\rm bar}$ is a parameter that defines the shape of bar profiles. The function is only defined out to $r_{\rm out}$, which is the bar radius. Beyond $r_{\rm out}$, $\mu_{\rm bar}$ is set to 0. Kim et al. (2012) compared their hydrodynamical simulations of galaxies that have a bulge with the observational study of Comerón et al. (2010)[26] and show that observed bars are best represented by $m_{\rm bar} \leqslant 0.5$.

It would be instructive to compare the two functions (Sérsic and Ferrers profile) for the fits. However, it is not straightforward to convert Sérsic indices to the $m_{\rm bar}$. Therefore, to compare $n_{\rm bar}$ and $m_{\rm bar}$, we ran GALFIT (version 3.0.5; Peng et al. 2002, 2010) on the bar model images that were obtained with BUDDA in order to estimate parameters of the Ferrers profile. GALFIT presents the modified Ferrers profile that has the following functional form:

$$\mu_{\rm bar}(r) = \mu_0(1-(r/r_{\rm out})^{2-\beta})^{\alpha}, \quad (4)$$

where μ_0 is the central surface brightness, α describes how sharply the bar profile drops near $r_{\rm out}$, and β describes the inner central slope of the profile. Because of its ability to describe a flat core and sharp truncation, the modified Ferrers profile is often used to model bars or lenses (Peng et al. 2010). We refer the readers to Figure 4 of Peng et al. (2010) for details about the profiles.

[26] A total of 90% of their sample galaxies have Hubble T $\leqslant$ 4 (SBbc).

Parameters of the Ferrers function and modified Ferrers function are different in a way that $\alpha = m_{\rm bar} - 0.5$, and β is fixed to 0 in the Ferrers function. But as we will see in Figure 5, many of our bar models, especially those that have no bulge, do not have $\beta = 0$.

We compare α and $n_{\rm bar}$ and β and $n_{\rm bar}$ in Figure 5. For 35 of the 144 galaxies GALFIT did not converge to a meaningful solution, and for those we were not able to obtain α and β values. As we expected, $n_{\rm bar}$ and β are strongly related, and $n_{\rm bar}$ and α also show a correlation. Flat bars ($n_{\rm bar} < 0.4$) mostly have $\beta < 0.5$ and $\alpha \leqslant 1.0$, whereas the exponential bars have $\beta > 0.5$. Therefore, both Sérsic and modified Ferrers profiles can describe the degree of flatness, and our results from the previous section are insensitive to the choice of fitting functions.

4. THE GLOBAL SHAPE OF BARS

Previous observational studies, which were primarily in the optical, found rectangular-shaped bars in strongly barred early-type galaxies (Athanassoula et al. 1990) and galaxies with classical and disky pseudobulges (Gadotti 2011). We now revisit this topic using our MIR data and the detailed decompositions with BUDDA.

Simulations predict that bars are rectangular in shape (Athanassoula et al. 1990; Athanassoula & Misiriotis 2002; Scannapieco & Athanassoula 2012). The manifold theoretical model (Romero-Gómez et al. 2006, 2007; Athanassoula 2012; Athanassoula et al. 2010), which has been proposed to explain the formation and structure of rings and spiral arms in barred galaxy potentials, argues that orbits of confined chaos play a crucial role in explaining the rectangular shape of bars (Athanassoula et al. 2010). In particular, the manifold branches produce the building blocks of the rectangular outline of the outer parts of a strong bar.

As discussed in Section 2.2, the generalized ellipse equation (Equation (2)) has an exponent "c", the shape parameter, which can distinguish between diamond-shaped and disky, rectangular and boxy, and an elliptical shape. To help the reader visualize the different shapes, we show three different shapes of the bar models in Figure 6. In this study, we model the outermost, global shape of the bar.

In Figure 7 we show the distribution of the global bar shape parameter (c) of all the bars we fit for this study. All bars are boxy and have a shape parameter c greater than 2. There are *no disky bars* in our sample. We find no significant differences in the global shape of bars with different bulge types—the median bar shape for all B/T and all three bulge types agrees within one standard deviation of the distributions. The Kolmogorov–Smirnov test confirms that we cannot rule out a null hypothesis that the bar shapes of groups shown in Figure 7 are drawn from the same parent population with the smallest probability, $P \sim 0.15$.

Athanassoula et al. (1990) measured shape parameters as a function of bar radius for 12 galaxies. We compare our global shape parameters from the BUDDA fit and those of Athanassoula et al. (1990) for five galaxies in common and find that our global shape parameters correspond to the shape parameter at 0.9–1.1 of the bar length that Athanassoula et al. (1990) obtained. The robustness of bar shape parameter obtained with BUDDA has been tested in Gadotti (2008), but we also have tested on artificial galaxies of various effective radii and Sérsic indices. We find that the shape parameters estimated from BUDDA agree within 10% of the input value.

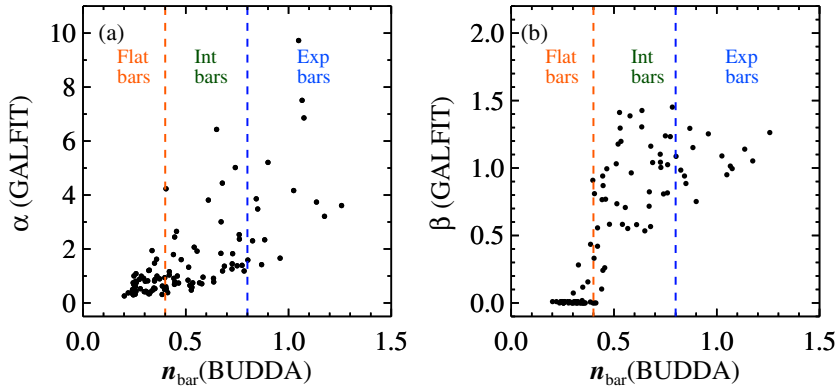

Figure 5. Comparisons of bar radial profile parameters; bar Sérsic index (n_{bar}) from the Sérsic profile fit, and α and β from the modified Ferrers function (Equation (4)).

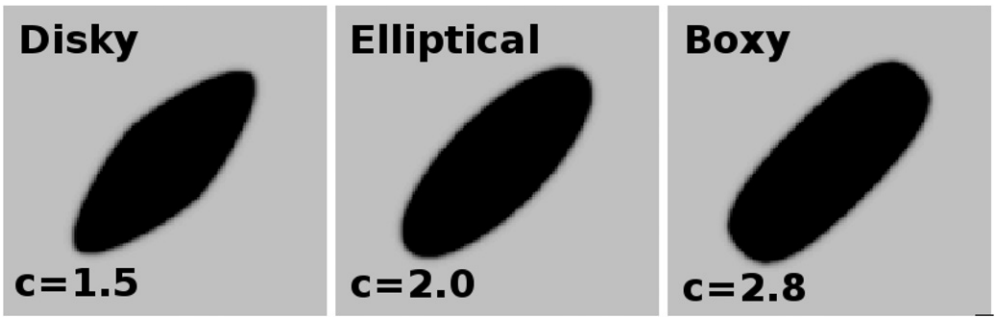

Figure 6. Morphology of bars that are simulated with BUDDA. From left to right, we plot disky, elliptical, and boxy shapes of bars. The shape parameter "c" from Equation (2) is written in the bottom left corner for each panel. All bars have ellipticity ($1 - b/a$) of 0.65.

Simulations agree with the data that bars are boxy (e.g., Athanassoula et al. 1990, 2010; Athanassoula & Misiriotis 2002; Scannapieco & Athanassoula 2012). In addition to what Athanassoula et al. (1990) found for strongly barred early-type galaxies and Gadotti (2011) found for classical and disky pseudobulge galaxies, we find that bars are rectangular even in late-type disk galaxies.

One caveat is that we fit the bar with a single component. However, bars are known to experience a buckling instability in which the central regions of the bar puff up and extend vertically out from the disk plane. This has been observed as a peanut-shaped or X-shaped feature in some edge-on galaxies (Jarvis 1986; Lütticke et al. 2000). Even in some moderately face-on galaxies, central parts of bars appear boxy over a region where the buckling instability has occurred (Athanassoula & Beaton 2006; Erwin & Debattista 2013), and this is observed as a bar lens seen face-on (Athanassoula et al. 2014; Laurikainen et al. 2014). Detailed study on the shape of these two different structures of the bar will be performed in the near future.

5. DISCUSSION

5.1. Bar Profiles

Several ideas have been proposed for the different radial light profiles of bars. Combes & Elmegreen (1993) suggested that bars in early- and late-type spiral galaxies have resonances at different locations and that this leads to the different light profiles. They also suggested that the flat profiles along the bar in early-type disk galaxies are due to an inner Lindblad resonance that is absent in late-type galaxies. Quillen (1996) suggested that bars in early-type spirals have a flat surface brightness profile because the ellipticities of the main bar orbits change rapidly as they approach corotation near the bar end, while bars in late-type galaxies show exponential profiles because the resonances are more spread out. Elmegreen et al. (1996) suggest that flat profiles of bars originated from the excessive stars at the bar ends where the orbits crowd near the inner 4:1 resonance. However, late-type bars do not show such resonance crowding (Elmegreen et al. 1996).

Some models find that bars end near the 4:1 resonance (Contopoulos et al. 1989; Athanassoula 1992a; Quillen et al. 1994; Skokos et al. 2002) and corotation radius is an upper limit of the bar extent (Contopoulos 1980; Sellwood & Wilkinson 1993). However, Elmegreen et al. (1996) claim that bars end at no specific resonance, but end in the region covered by many resonances in the range from inner 4:1 to corotation resonance. If the 4:1 and corotation resonances are located close to each other, stellar orbits crowd together between these two resonances. Therefore, it may produce a bar with a nearly constant light distribution, i.e., a flat bar. Such a crowding of resonances mostly occurs in bright, massive galaxies, i.e., in early-type disk galaxies, where the $\Omega - \kappa/2$ has large maxima and therefore bars can be formed with a large pattern speed (Combes & Elmegreen 1993). However, in late-type disks, $\Omega - \kappa/2$ has low values as a whole, and the bar pattern speed is low, locating the corotation radius further out in the disk. So this crowding of resonances would develop early-type bars with flat surface brightness profiles.

N-body simulations of disk galaxies with different central dark matter halo concentrations have shown that there are differences in the mass density profiles of bars (Athanassoula & Misiriotis 2002). Bars in galaxies with centrally concentrated halos (MH model of Athanassoula & Misiriotis 2002) show a flat mass density profile followed by a steeply decreasing density profile toward the end of the bar—this is similar to the S^4G bars in bulge-dominated galaxies in our sample. In the future

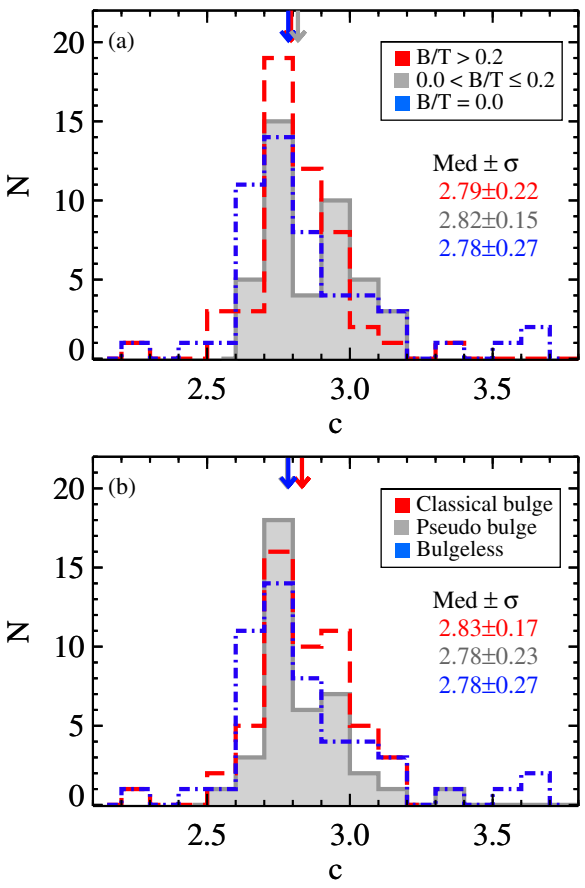

Figure 7. Distribution of the bar shape parameter (c from Equation (2)) in the generalized ellipse fit for different types of galaxies. Median shape parameters for each group are plotted with downward-pointing arrows. (a) Galaxies are divided by B/T: B/T > 0.2 (dashed lines), 0.0 < B/T ⩽ 0.2 (solid lines), and B/T = 0.0 (dot–dashed lines). (b) Galaxies are divided by bulge types: classical bulge galaxies (dashed lines), pseudobulge galaxies (solid lines), and bulgeless galaxies (dot–dashed lines).

perhaps high-resolution simulation kinematic data will help us test whether the dark matter halos predicted by the simulations are borne out in these galaxies.

Some caveats should be considered. In this study, we assumed that a bar forms in a disk that shows an exponential profile. However, the underlying profile of disks may evolve with redshift. For example, half-mass radii change with redshift (e.g., Dutton et al. 2011). Nevertheless, these changes are slow up to $z = 1$–1.5, and a recent study (Kraljic et al. 2012) claims that bars start to form around this epoch. Thus, we expect that the impact of intrinsic change of disk profiles would be limited at $z < 1$–1.5.

Disk galaxies at $z > 1$–1.5 are found to be compact (van Dokkum et al. 2008; van der Wel et al. 2011). Such galaxies exhibit a similar Sérsic index distribution to that of the massive ($M_* > 10^{11}\ M_\odot$) local disk galaxies, though the mean Sérsic index of high-z disk galaxies is a bit larger (Chevance et al. 2012). Most disk galaxies in this mass range today are found to host a bar; thus, those compact disk galaxies are expected to form a bar by $z = 0$. If a bar forms in such a compact, exotic galaxy at an early epoch, it may take longer to change the bar light profile to a flat one. Depending on the initial condition of disk profiles, this may induce a scatter among high-z progenitors. Thus, if profiles of disks vary among galaxies when bars form, our results on bar profiles might also be affected.

5.2. Bar Profile Bimodality?

In Section 3 we show that surface brightness profiles of bars change with stellar mass. Among less massive galaxies ($M_*/M_\odot \leqslant 10^{10}$), most of the galaxies show steeply decreasing exponential profiles. On the other hand, flat bars are dominant in massive galaxies ($M_*/M_\odot > 10^{10}$). The transition from exponential to flat profile occurs at $M_{3.6\ \mu\mathrm{m}} \sim -20$ mag ($M_*/M_\odot \sim 10^{10.2}$).

Interestingly, this is the characteristic mass where the bar fraction is at its minimum (Nair & Abraham 2010) and close to the characteristic mass that corresponds to the rotation velocity ($V_c \sim 120$ km s^{-1}; see Comerón et al. 2014), where vertical structures of interstellar medium (ISM)traced by dust morphology show a transition (Dalcanton et al. 2004; Yoachim & Dalcanton 2006). Also, it is close to the characteristic mass where the mass-to-light ratios of thin and thick disks change (Comerón et al. 2011), and galaxy properties such as age of stellar populations, surface mass density, and concentration show bimodality (Kauffmann et al. 2003). Related to this, galaxy color (Strateva et al. 2001; Baldry et al. 2004), luminosity (Balogh et al. 2004), and size (Shen et al. 2003) are also found to show bimodal distributions.

This suggests that the mechanism that changes bar profiles from exponential to flat may also be associated with global properties of their host galaxies such as galaxy mass, color, size, and also distribution of dust lanes that are related to disk instability (Dalcanton et al. 2004).

5.3. Are Bars Robust or Recurrent?

The result that high-B/T galaxies do not have an exponential bar implies that such galaxies did not dissolve a preexisting bar and did not build a new one. Some studies have argued that the central mass concentration can destroy bars (e.g., Hasan & Norman 1990; Hasan et al. 1993; Norman et al. 1996). If bars in such high-B/T galaxies are destroyed and formed again, at least some bars should exhibit an exponential bar profile even among high-B/T galaxies. However, we do not see any in our study. Simulations find that with the central mass concentration, the strength of the bar decreases (e.g., Shen & Sellwood 2004; Athanassoula et al. 2005). However, to be able to completely destroy a bar, the mass concentration has to be either highly concentrated, whose scale length is less than a few parsecs, or massive enough, at least several percent of the disk mass (Shen & Sellwood 2004; Athanassoula et al. 2005; Debattista et al. 2006). For the same central mass concentration, Athanassoula et al. (2005) find that bars with an exponential surface density profile can be dissolved, while strong bars with a flat surface density profile witness only a decrease of their strength. This is consistent with our results that higher-B/T galaxies only shows flat bars, and this implies that at least bars in galaxies with a big central bulge (high B/T) are *not* recurrent.

5.4. The Invariant Bar Shape and the Bar Profile: An Indicator of Bar Age?

We find that the global shapes of bars do not vary across galaxy mass or bulge dominance. This suggests that either (1) through the bar formation phase and secular evolutionary phase, the global shapes of bars do not change much; or (2) the global shapes of bars evolve to have similar shapes. However, the change in the surface brightness profile from exponential to flat suggests that there is evolution in the number of stars that are trapped in the bar orbits (Sellwood & Wilkinson 1993;

Sellwood 2013; Athanassoula 2003, 2013). Because bars are formed out of disk material, we can assume that the light profile of the bar would be exponential-like when they just formed. However, as a galaxy ages and the bar evolves, the galaxy would have enough time to experience resonance crowding (Combes & Elmegreen 1993) and trap stars into the bar orbit, and thus the bar becomes longer and stronger (Sellwood & Wilkinson 1993; Athanassoula & Misiriotis 2002; Athanassoula 2013; Sellwood 2013). This will lead bars to have a flat profile. Therefore, it is reasonable that the light profile of the bar will change from an initial exponential profile to a flatter profile.

This fits in well with our understanding of the cosmological evolution of disks and bars. The fraction of bars in L^* and brighter galaxies is found to evolve such that it increases from $z = 0.85$ to the present day (Abraham et al. 1999; Jogee et al. 2004; Sheth et al. 2008; Cameron et al. 2010; Kraljic et al. 2012; Melvin et al. 2014). Moreover, these studies have shown that the bar fraction is the highest in the most massive, bulge-dominated, red galaxies at high redshifts with little evolution in this population over the past 7 Gyr of cosmic time. This is perfectly consistent with this study. We find that massive, bulge-dominated galaxies have flat bars as one would expect if these bars have been in existence for several gigayears and dynamically more evolved. Interestingly, this is also consistent with the result of Holwerda et al. (2012) that dust lanes in edge-on galaxies have been in existence since $z \sim 0.8$ in massive galaxies. This can be interpreted such that massive galaxies had enough time to dynamically evolve so that cold ISM can sink into the galactic plane to form the dust lane (Dalcanton et al. 2004).

In low-mass, disk-dominated blue galaxies, studies show that the fraction of bars evolves gradually, increasing the present-day fraction over time (Abraham et al. 1999; Sheth et al. 2008; Cameron et al. 2010; Melvin et al. 2014). This means that some low-mass systems had their bars early but more and more of them acquired bars over the past 7 Gyr of evolutionary time. Therefore, today we might expect a larger spread in the bar profile with more exponential profiles in the late-type galaxies, as we see from the analysis presented here. Thus, it stands to reason that if we could ascertain bar profile evolution with time, then we might be able to age-date a bar. However, the rate of capturing stars onto bar orbits may itself evolve in time owing to minor mergers, star formation, and other processes, so the age indicator may still remain elusive.

There have been several studies to infer various ages of bars—using the vertical velocity dispersion (σ_z) of bars (Gadotti & de Souza 2005), comparing gas mass with gas accretion rate in the bar region (Elmegreen et al. 2009), and age of stellar populations in bars (Sánchez-Blázquez et al. 2011). However, we should be careful what we call the bar age. As bars are built out of disk stars and gas, the time elapsed since the formation of bar structure is not necessarily the same as the age of stellar populations that make up the bar.

Although the exact time since the bar formation cannot currently be easily determined, it is certainly a very important parameter to measure in order to understand the impact of bars in galaxy evolution. We expect that the flatness of the bar profile, combined with theoretical work, can be helpful in devising a way to measure the "dynamical age" of the bar. We expect that, in general, more dynamically evolved bars should have a flatter surface brightness profile, and we have presented the observational evidence that this is indeed the case.

5.5. Necessity for Cosmic Gas Accretion?

Previous studies have shown that the formation epoch of bars is correlated with the galaxy host properties—in other words, the more massive, bulge-dominated, early-type disk galaxies formed their bars early (at $z \gtrsim 1$, Sheth et al. 2008; Cameron et al. 2010; Kraljic et al. 2012; Melvin et al. 2014). Once formed, bars are resilient and are not likely destroyed easily (e.g., Athanassoula 2003; Athanassoula et al. 2013; Romano-Díaz et al. 2008) without major mergers.

At the same time, many barred spiral galaxies contain molecular gas within the bar radius (e.g., Sakamoto et al. 1999; Sheth et al. 2002, 2005). This is surprising given that bars in early-type galaxies have likely been in existence since $z \sim 1$ ($\sim$8 Gyr). Elmegreen et al. (2009) have argued that the ratio of the gas mass divided by the gas accretion rate may be used as an age for the bar. Typical disk gas surface densities in nearby spiral disks are $\sim$5–10 $M_\odot$ pc^{-2} (Young et al. 1995; Sheth et al. 2005). Typical bar radius is $\sim$2.5 kpc (Erwin 2005). Therefore, one expects the total gas mass inside the bar corotation of $\sim 10^9\ M_\odot$. Then all the gas within the bar corotation radius should be deposited into the inner Lindblad resonance region within $\sim$1 Gyr if we assume the gas inflow rate of 1 $M_\odot$ yr^{-1}. Indeed, with a detailed estimate, Elmegreen et al. (2009) argue that the bar in NGC 1365 is not much older than 1–2 Gyr.

For barred galaxies, gas within the bar corotation radius is driven inward, and gas outside the corotation radius is driven outward. Thus, in-plane accretion can only come from around the end of the bar region, except for a special case.[27] Then how can there be molecular gas in these bars if we have a finite reservoir of gas and a star formation rate in the bar region? We argue that the gas might have been replenished via cosmic gas accretion (e.g., Sancisi et al. 2008; Dekel et al. 2009; Fraternali & Binney 2006; Fraternali 2014; Silk & Mamon 2012; Combes 2014) for these barred galaxies. In general, gas in spiral galaxies can be replenished from outer disks where there is lots of gas that can come inward from spiral torques. However, for barred spiral galaxies the amount of gas that can be transported inward is limited. Therefore, we indeed need cosmic gas accretion to sustain bars and allow them to grow slowly over time. This is consistent with the results from cosmological simulations of Kraljic et al. (2012), which expect slow emergence of bars from $z \sim 1$, and the slowdown of the bar growth in the presence of gas (Athanassoula et al. 2013). Lastly, such cosmic accretion might be the origin of the gas that brings galaxies to evolve and renew bars (Bournaud & Combes 2002; Block et al. 2002).

6. SUMMARY AND CONCLUSIONS

We make use of 2D image decompositions on 144 barred galaxies of Hubble types from SB0 to SBdm using 3.6 μm images drawn from the S^{4}G. We investigate the structural properties of bars, in particular radial light profiles of bars and 2D global shapes of bars. We summarize our results as follows.

1. We quantify the surface brightness profile of bars by fitting bar isophotes with the Sérsic profile. We find that massive, higher-B/T, and classical bulge galaxies tend to have flat bars, while less massive and bulgeless galaxies tend to show steeply decreasing exponential bar profiles. We find that whenever there is a bulge, galaxies tend to have flat bars.

[27] If the spiral arm and bar are connected and their pattern speeds match, gas could be transported inward from the outer disk via spiral arms and drive episodic fueling from the outer disk (Sheth et al. 2005).

2. We model the global shape of bars with generalized ellipses. All bars are found to be rectangular-like, i.e., boxy. There are no significant differences in the shape of bars among galaxies. This implies that as bars evolve, light profiles of bars change from exponential to flat, although their outermost shapes remain boxy.
3. We conjecture that at earlier evolutionary stages, the bar profile resembles that of the disk that shows an exponential profile ($\langle n_{\rm bar} \rangle \sim 1$). But as galaxies evolve, bars become stronger, and this leads to the development of flatter profiles. In this regard, our findings are consistent with the cosmological evolution of barred galaxies, which predicts that more massive, bulge-dominated, red disk galaxies formed their bars first and thus had enough time for their bars to evolve toward flat profiles. Combined with theoretical works and simulations, we will be able to diagnose the dynamical status of bars using light profiles of bars.
4. Cosmic gas accretion is strongly required to explain the presence of gas and star formation within bar regions for barred galaxies that have been in existence for more than their gas consumption timescale (∼1–2 Gyr).

We thank Frederic Bournaud, the referee, for insightful comments that greatly improved this paper. The authors thank the S^{4}G team for their effort in this project. T.K. is grateful to Woong-Tae Kim and his research group for their helpful comments and discussions. T.K., K.S., J.-C.M.-M., and T.M. acknowledge support from the National Radio Astronomy Observatory. The National Radio Astronomy Observatory is a facility of the National Science Foundation operated under cooperative agreement by Associated Universities, Inc. We are grateful for the support from NASA JPL/Spitzer grant RSA 1374189 provided for the S^{4}G project. T.K. and M.G.L. were supported by the National Research Foundation of Korea (NRF) grant funded by the Korea Government (MEST; No. 2012R1A4A1028713). T.K. acknowledges the support from ESO for the studentship in 2011–2012. D.A.G. acknowledges funding under the Marie Curie Actions of the European Commission (FP7-COFUND). E.A. and A.B. thank the Centre National d'Etudes Spatiales for financial support. We acknowledge financial support from the People Programme (Marie Curie Actions) of the European Union's FP7/2007-2013/ to the DAGAL network under REA grant agreement No. PITN-GA- 2011-289313. L.C.H acknowledges support by the Chinese Academy of Science through grant No. XDB09030102 (Emergence of Cosmological Structures) from the Strategic Priority Research Program and by the National Natural Science Foundation of China through grant No. 11473002. This research is based on observations and archival data made with the *Spitzer Space Telescope* and made use of the NASA/IPAC Extragalactic Database (NED), which are operated by the Jet Propulsion Laboratory, California Institute of Technology, under a contract with the National Aeronautics and Space Administration (NASA). We acknowledge the usage of the HyperLeda database (http://leda.univ-lyon1.fr).

Facility: Spitzer

REFERENCES

Abraham, R. G., Merrifield, M. R., Ellis, R. S., Tanvir, N. R., & Brinchmann, J. 1999, MNRAS, 308, 569
Arsenault, R. 1989, A&A, 217, 66
Athanassoula, E. 1992a, MNRAS, 259, 328
Athanassoula, E. 1992b, MNRAS, 259, 345
Athanassoula, E. 2002, ApJL, 569, L83
Athanassoula, E. 2003, MNRAS, 341, 1179
Athanassoula, E. 2005, MNRAS, 358, 1477
Athanassoula, E. 2012, MNRAS, 426, L46
Athanassoula, E. 2013, in Bars and Secular Evolution in Disk Galaxies: Theoretical Input, ed. J. Falcón-Barroso & J. H. Knapen (Cambridge: Cambridge Univ. Press), 305
Athanassoula, E., & Beaton, R. L. 2006, MNRAS, 370, 1499
Athanassoula, E., Lambert, J. C., & Dehnen, W. 2005, MNRAS, 363, 496
Athanassoula, E., Laurikainen, E., Salo, H., & Bosma, A. 2014, arXiv:1405.6726
Athanassoula, E., Machado, R. E. G., & Rodionov, S. A. 2013, MNRAS, 429, 1949
Athanassoula, E., & Misiriotis, A. 2002, MNRAS, 330, 35
Athanassoula, E., Morin, S., Wozniak, H., et al. 1990, MNRAS, 245, 130
Athanassoula, E., Romero-Gómez, M., Bosma, A., & Masdemont, J. J. 2009a, MNRAS, 400, 1706
Athanassoula, E., Romero-Gómez, M., Bosma, A., & Masdemont, J. J. 2010, MNRAS, 407, 1433
Athanassoula, E., Romero-Gómez, M., & Masdemont, J. J. 2009b, MNRAS, 394, 67
Baldry, I. K., Glazebrook, K., Brinkmann, J., et al. 2004, ApJ, 600, 681
Balogh, M. L., Baldry, I. K., Nichol, R., et al. 2004, ApJL, 615, L101
Baumgart, C. W., & Peterson, C. J. 1986, PASP, 98, 56
Begelman, M. C., & Shlosman, I. 2009, ApJL, 702, L5
Block, D. L., Bournaud, F., Combes, F., Puerari, I., & Buta, R. 2002, A&A, 394, L35
Böker, T., Laine, S., van der Marel, R. P., et al. 2002, AJ, 123, 1389
Böker, T., Sarzi, M., McLaughlin, D. E., et al. 2004, AJ, 127, 105
Böker, T., Schinnerer, E., & Lisenfeld, U. 2011, A&A, 534, A12
Bournaud, F., & Combes, F. 2002, A&A, 392, 83
Buta, R., Block, D. L., & Knapen, J. H. 2003, AJ, 126, 1148
Buta, R., & Combes, F. 1996, FCPh, 17, 95
Buta, R. J., Knapen, J. H., Elmegreen, B. G., et al. 2009, AJ, 137, 4487
Buta, R. J., Sheth, K., Regan, M., et al. 2010, ApJS, 190, 147
Buta, R., et al. 2014, ApJS, submitted
Cameron, E., Carollo, C. M., Oesch, P., et al. 2010, MNRAS, 409, 346
Chevance, M., Weijmans, A.-M., Damjanov, I., et al. 2012, ApJL, 754, L24
Cisternas, M., Gadotti, D. A., Knapen, J. H., et al. 2013, ApJ, 776, 50
Coelho, P., & Gadotti, D. A. 2011, ApJL, 743, L13
Combes, F. 2008, in IAU Symp. 245, Formation and Evolution of Galaxy Bulges, ed. M. Bureau, E. Athanassoula, & B. Barbuy (Cambridge: Cambridge Univ. Press), 151
Combes, F. 2014, in ASP Conf. Ser. 480, Structure and Dynamics of Disk Galaxies, ed. M. S. Seigar & P. Treuthardt (San Francisco, CA: ASP), 211
Combes, F., & Elmegreen, B. G. 1993, A&A, 271, 391
Comerón, S., Elmegreen, B. G., Knapen, J. H., et al. 2011, ApJ, 741, 28
Comerón, S., Elmegreen, B. G., Salo, H., et al. 2012, ApJ, 759, 98
Comerón, S., Elmegreen, B. G., Salo, H., et al. 2014, A&A, 571, 58
Comerón, S., Knapen, J. H., Beckman, J. E., et al. 2010, MNRAS, 402, 2462
Contopoulos, G. 1980, A&A, 81, 198
Contopoulos, G., Gottesman, S. T., Hunter, J. H., Jr., & England, M. N. 1989, ApJ, 343, 608
Dalcanton, J. J., Yoachim, P., & Bernstein, R. A. 2004, ApJ, 608, 189
de Jong, R. S. 1996, A&AS, 118, 557
de Souza, R. E., Gadotti, D. A., & dos Anjos, S. 2004, ApJS, 153, 411
Debattista, V. P., Mayer, L., Carollo, C. M., et al. 2006, ApJ, 645, 209
Debattista, V. P., & Sellwood, J. A. 1998, ApJL, 493, L5
Dekel, A., Birnboim, Y., Engel, G., et al. 2009, Natur, 457, 451
Devereux, N. 1987, ApJ, 323, 91
Durbala, A., Sulentic, J. W., Buta, R., & Verdes-Montenegro, L. 2008, MNRAS, 390, 881
Dutil, Y., & Roy, J.-R. 1999, ApJ, 516, 62
Dutton, A. A., van den Bosch, F. C., Faber, S. M., et al. 2011, MNRAS, 410, 1660
Ellison, S. L., Nair, P., Patton, D. R., et al. 2011, MNRAS, 416, 2182
Elmegreen, B. G., & Elmegreen, D. M. 1985, ApJ, 288, 438
Elmegreen, B. G., Elmegreen, D. M., Chromey, F. R., Hasselbacher, D. A., & Bissell, B. A. 1996, AJ, 111, 2233
Elmegreen, B. G., Galliano, E., & Alloin, D. 2009, ApJ, 703, 1297
Erwin, P. 2005, MNRAS, 364, 283
Erwin, P., Beckman, J. E., & Pohlen, M. 2005, ApJL, 626, L81
Erwin, P., & Debattista, V. P. 2013, MNRAS, 431, 3060
Erwin, P., Pohlen, M., & Beckman, J. E. 2008, AJ, 135, 20
Eskew, M., Zaritsky, D., & Meidt, S. 2012, AJ, 143, 139
Falcón-Barroso, J., & Knapen, J. H. 2013, Secular Evolution of Galaxies (Cambridge: Cambridge Univ. Press)

Fathi, K., Allen, M., Boch, T., Hatziminaoglou, E., & Peletier, R. F. 2010, MNRAS, 406, 1595
Fazio, G. G., Hora, J. L., Allen, L. E., et al. 2004, ApJS, 154, 10
Fisher, D. B., & Drory, N. 2008, AJ, 136, 773
Fraternali, F. 2014, in IAU Symp. 298, Setting the Scene for Gaia and LAMOST, ed. S. Feltzing, G. Zhao, N. A. Walton, & P. Whitelock (Cambridge: Cambridge Univ. Press), 228
Fraternali, F., & Binney, J. J. 2006, MNRAS, 366, 449
Gadotti, D. A. 2008, MNRAS, 384, 420
Gadotti, D. A. 2009, MNRAS, 393, 1531
Gadotti, D. A. 2011, MNRAS, 415, 3308
Gadotti, D. A., Baes, M., & Falony, S. 2010, MNRAS, 403, 2053
Gadotti, D. A., & de Souza, R. E. 2005, ApJ, 629, 797
Gadotti, D. A., & dos Anjos, S. 2001, AJ, 122, 1298
Gutiérrez, L., Erwin, P., Aladro, R., & Beckman, J. E. 2011, AJ, 142, 145
Hasan, H., & Norman, C. 1990, ApJ, 361, 69
Hasan, H., Pfenniger, D., & Norman, C. 1993, ApJ, 409, 91
Hawarden, T. G., Mountain, C. M., Leggett, S. K., & Puxley, P. J. 1986, MNRAS, 221, 41P
Ho, L. C., Filippenko, A. V., & Sargent, W. L. W. 1997, ApJ, 487, 591
Holwerda, B. W., Dalcanton, J. J., Radburn-Smith, D., et al. 2012, ApJ, 753, 25
Holwerda, B. W., González, R. A., van der Kruit, P. C., & Allen, R. J. 2005, A&A, 444, 109
Hunt, L. K., & Malkan, M. A. 1999, ApJ, 516, 660
Hunter, D. A., & Elmegreen, B. G. 2006, ApJS, 162, 49
Jarvis, B. J. 1986, AJ, 91, 65
Jogee, S., Barazza, F. D., Rix, H.-W., et al. 2004, ApJL, 615, L105
Kauffmann, G., Heckman, T. M., White, S. D. M., et al. 2003, MNRAS, 341, 54
Kelvin, L. S., Driver, S. P., Robotham, A. S. G., et al. 2012, MNRAS, 421, 1007
Kim, T., Gadotti, D. A., Sheth, K., et al. 2014, ApJ, 782, 64
Kim, W.-T., Seo, W.-Y., & Kim, Y. 2012, ApJ, 758, 14
Knapen, J. H., Beckman, J. E., Heller, C. H., Shlosman, I., & de Jong, R. S. 1995, ApJ, 454, 623
Knapen, J. H., Pérez-Ramírez, D., & Laine, S. 2002, MNRAS, 337, 808
Knapen, J. H., Shlosman, I., & Peletier, R. F. 2000, ApJ, 529, 93
Kormendy, J., & Kennicutt, R. C., Jr. 2004, ARA&A, 42, 603
Kraljic, K., Bournaud, F., & Martig, M. 2012, ApJ, 757, 60
Kubryk, M., Prantzos, N., & Athanassoula, E. 2013, MNRAS, 436, 1479
Laine, J., Laurikainen, E., Salo, H., et al. 2014, MNRAS, 441, 1992
Laine, S., Shlosman, I., Knapen, J. H., & Peletier, R. F. 2002, ApJ, 567, 97
Lansbury, G. B., Lucey, J. R., & Smith, R. J. 2014, MNRAS, 439, 1749
Laurikainen, E., & Salo, H. 2002, MNRAS, 337, 1118
Laurikainen, E., Salo, H., Athanassoula, E., Bosma, A., & Herrera-Endoqui, M. 2014, MNRAS, 444, L80
Laurikainen, E., Salo, H., & Buta, R. 2004a, ApJ, 607, 103
Laurikainen, E., Salo, H., & Buta, R. 2005, MNRAS, 362, 1319
Laurikainen, E., Salo, H., Buta, R., & Knapen, J. H. 2007, MNRAS, 381, 401
Laurikainen, E., Salo, H., Buta, R., & Knapen, J. H. 2011, MNRAS, 418, 1452
Laurikainen, E., Salo, H., Buta, R., Knapen, J. H., & Comerón, S. 2010, MNRAS, 405, 1089
Laurikainen, E., Salo, H., Buta, R., & Vasylyev, S. 2004b, MNRAS, 355, 1251
Lee, G.-H., Woo, J.-H., Lee, M. G., et al. 2012, ApJ, 750, 141
Lütticke, R., Dettmar, R.-J., & Pohlen, M. 2000, A&AS, 145, 405
Maltby, D. T., Gray, M. E., Aragón-Salamanca, A., et al. 2012a, MNRAS, 419, 669
Maltby, D. T., Hoyos, C., Gray, M. E., Aragón-Salamanca, A., & Wolf, C. 2012b, MNRAS, 420, 2475
Marinova, I., & Jogee, S. 2007, ApJ, 659, 1176
Martin, P. 1995, AJ, 109, 2428
Martin, P., & Roy, J.-R. 1994, ApJ, 424, 599
Martín-Navarro, I., Bakos, J., Trujillo, I., et al. 2012, MNRAS, 427, 1102
Martinez-Valpuesta, I., Shlosman, I., & Heller, C. 2006, ApJ, 637, 214
Martini, P., Regan, M. W., Mulchaey, J. S., & Pogge, R. W. 2003, ApJ, 589, 774
McLeod, K. K., & Rieke, G. H. 1995, ApJ, 441, 96
Meidt, S. E., Schinnerer, E., Knapen, J. H., et al. 2012a, ApJ, 744, 17
Meidt, S. E., Schinnerer, E., Muñoz-Mateos, J.-C., et al. 2012b, ApJL, 748, L30
Melvin, T., Masters, K., Lintott, C., et al. 2014, MNRAS, 438, 2882
Menéndez-Delmestre, K., Sheth, K., Schinnerer, E., Jarrett, T. H., & Scoville, N. Z. 2007, ApJ, 657, 790
Moles, M., Marquez, I., & Perez, E. 1995, ApJ, 438, 604
Mulchaey, J. S., & Regan, M. W. 1997, ApJL, 482, L135
Muñoz-Mateos, J. C., Sheth, K., Gil de Paz, A., et al. 2013, ApJ, 771, 59
Nair, P. B., & Abraham, R. G. 2010, ApJL, 714, L260
Norman, C. A., Sellwood, J. A., & Hasan, H. 1996, ApJ, 462, 114
Pastrav, B. A., Popescu, C. C., Tuffs, R. J., & Sansom, A. E. 2013, A&A, 553, A80
Peng, C. Y., Ho, L. C., Impey, C. D., & Rix, H.-W. 2002, AJ, 124, 266
Peng, C. Y., Ho, L. C., Impey, C. D., & Rix, H.-W. 2010, AJ, 139, 2097
Pérez, I., & Sánchez-Blázquez, P. 2011, A&A, 529, A64
Pohlen, M., Dettmar, R.-J., Lütticke, R., & Aronica, G. 2002, A&A, 392, 807
Pohlen, M., & Trujillo, I. 2006, A&A, 454, 759
Quillen, A. C. 1996, arXiv:astroph/96090141
Quillen, A. C., Frogel, J. A., & Gonzalez, R. A. 1994, ApJ, 437, 162
Radburn-Smith, D. J., Roškar, R., Debattista, V. P., et al. 2012, ApJ, 753, 138
Regan, M. W., & Elmegreen, D. M. 1997, AJ, 114, 965
Regan, M. W., Sheth, K., & Vogel, S. N. 1999, ApJ, 526, 97
Romano-Díaz, E., Shlosman, I., Heller, C., & Hoffman, Y. 2008, ApJL, 687, L13
Romero-Gómez, M., Athanassoula, E., Masdemont, J. J., & García-Gómez, C. 2007, A&A, 472, 63
Romero-Gómez, M., Masdemont, J. J., Athanassoula, E., & García-Gómez, C. 2006, A&A, 453, 39
Saha, K., Martinez-Valpuesta, I., & Gerhard, O. 2012, MNRAS, 421, 333
Sakamoto, K., Okumura, S. K., Ishizuki, S., & Scoville, N. Z. 1999, ApJ, 525, 691
Salo, H., Laurikainen, E., Buta, R., & Knapen, J. H. 2010, ApJL, 715, L56
Sánchez, S. F., Rosales-Ortega, F. F., Iglesias-Páramo, J., et al. 2014, A&A, 563, A49
Sánchez, S. F., Rosales-Ortega, F. F., Marino, R. A., et al. 2012, A&A, 546, A2
Sánchez-Blázquez, P., Ocvirk, P., Gibson, B. K., Pérez, I., & Peletier, R. F. 2011, MNRAS, 415, 709
Sancisi, R., Fraternali, F., Oosterloo, T., & van der Hulst, T. 2008, A&ARv, 15, 189
Scannapieco, C., & Athanassoula, E. 2012, MNRAS, 425, L10
Sellwood, J. A. 1980, A&A, 89, 296
Sellwood, J. A. 2014, RvMP, 86, 1
Sellwood, J. A., & Wilkinson, A. 1993, RPPh, 56, 173
Seo, W.-Y., & Kim, W.-T. 2013, ApJ, 769, 100
Sérsic, J. L. 1963, BAAA, 6, 41
Sérsic, J. L., & Pastoriza, M. 1965, PASP, 77, 287
Shen, J., & Sellwood, J. A. 2004, ApJ, 604, 614
Shen, S., Mo, H. J., White, S. D. M., et al. 2003, MNRAS, 343, 978
Sheth, K., Elmegreen, D. M., Elmegreen, B. G., et al. 2008, ApJ, 675, 1141
Sheth, K., Regan, M., Hinz, J. L., et al. 2010, PASP, 122, 1397
Sheth, K., Regan, M. W., Vogel, S. N., & Teuben, P. J. 2000, ApJ, 532, 221
Sheth, K., Vogel, S. N., Regan, M. W., et al. 2002, AJ, 124, 2581
Sheth, K., Vogel, S. N., Regan, M. W., Thornley, M. D., & Teuben, P. J. 2005, ApJ, 632, 217
Silk, J., & Mamon, G. A. 2012, RA&A, 12, 917
Skokos, C., Patsis, P. A., & Athanassoula, E. 2002, MNRAS, 333, 861
Strateva, I., Ivezić, Ž., Knapp, G. R., et al. 2001, AJ, 122, 1861
Valenzuela, O., & Klypin, A. 2003, MNRAS, 345, 406
van der Wel, A., Rix, H.-W., Wuyts, S., et al. 2011, ApJ, 730, 38
van Dokkum, P. G., Franx, M., Kriek, M., et al. 2008, ApJL, 677, L5
Vika, M., Driver, S. P., Cameron, E., Kelvin, L., & Robotham, A. 2012, MNRAS, 419, 2264
Wang, J., Kauffmann, G., Overzier, R., et al. 2012, MNRAS, 423, 3486
Weinzirl, T., Jogee, S., Khochfar, S., Burkert, A., & Kormendy, J. 2009, ApJ, 696, 411
Yoachim, P., & Dalcanton, J. J. 2006, AJ, 131, 226
Young, J. S., Xie, S., Tacconi, L., et al. 1995, ApJS, 98, 219
Zaritsky, D., Kennicutt, R. C., Jr., & Huchra, J. P. 1994, ApJ, 420, 87